Magnetized Disk-Winds and the Origin of Bipolar Outflows

M. Camenzind

Landessternwarte Königstuhl, D-6900 Heidelberg, Fed. Rep. of Germany

Summary. Interstellar magnetic fields play certainly a distinct role in star formation and in galactic molecular disks. These magnetic fields are, however, also a key ingredient for accretion disks around young stellar objects and in the nuclei of galaxies. In these objects we find a strong observational link between accretion disks and bipolar outflows in the form of winds and jets.

In turbulent disks, the magnetic fields evolve according to the induction equation of mean field electrodynamics. In case of axisymmetric configurations, this leads to a coupled system of partial differential equations for the poloidal magnetic flux and the toroidal magnetic field including the effects of advection, spatial diffusion, differential rotation and helicity of the turbulence. In geometrically thin accretion disks, the lowest axisymmetric dynamo mode which can grow exponentially until equipartition with turbulence, is the quadrupolar field. Dipolar fields are found to decay exponentially.

The magnetic fields exterior to the disk have the structure of a rotating force-free magnetosphere. The shape of the poloidal field lines follows here from the solution of the relativistic Grad-Schlüter-Shafranov equation. The velocity and density in open magnetospheres is then essentially determined by the structure of the magnetic flux tubes. The luminosity of the wind is given by the magnetic luminosity of the disk surface. Magnetized winds ejected from the surface of the disk will be collimated by magnetic effects on scales typically larger than the light cylinder radius for these objects. The VLBI-jets of Quasars have therefore a radius of a fraction of a light year and reach a highly relativistic motion due to the extremely strong magnetization in the corona of the accretion disk. Protostellar jets have moderate velocities and jet radii of a few hundred AU.

1. Introduction

The various activities shown by young stellar objects (YSOs), some cataclysmic variables and LMXBs, and in particular by the nuclei of Quasars, Seyfert galaxies and radio galaxies are commonly attributed to the presence

of large accretion disks around the central mass condensations in these objects. There is a great similarity in the physics involved in these various objects, since the structure of steady accretion disks has a deep scaling behaviour in the sense that temperature, density and pressure in the disk scale appropriately with mass and accretion rate.

Magnetic fields play certainly some distinct role in star formation and galactic disks. But the great majority of accretion disk theory is still gas dynamical rather than magnetohydrodynamical. In contrast, our experience with turbulent space plasmas suggests that magnetic fields are of primary importance also for the theory of accretion disks. In this review talk, we briefly summarize the observational link between the existence of accretion disks and of bipolar outflows in the same type of objects. Large scale magnetic fields built up by the underlying accretion disk will launch a pair of bipolar outflows (or jets) normal to the disk. This is a natural explanation for the observed link between disks and bipolar outflows. The conditions for a possible amplification of magnetic fields in a disk are therefore crucial for the origin of bipolar outflows. We show in particular that dynamos acting in the boundary layer between the accretion disk and the central object are the most likely origin for these outflows and that the winds are driven away by strong toroidal magnetic fields in the boundary layer. Magnetic forces will collimate the outflows on scales much larger than the scale of the boundary layers, disk-winds are collimated into disk-jets. We show at the end that the optical jets observed in T Tauri stars are very similar to the parsec-scale radio jets of Quasars observed on the VLBI-scale – except for their velocities which only depend on the strength of the magnetization of the jet-plasma.

The importance of magnetic fields for accretion disks and the formation of jets has been discussed in various reviews which include Blandford (1989), Camenzind (1988, 1989a, b), Coroniti (1984), Königl (1989), Pudritz (1989), Zeldovich, Ruzmaikin and Sokoloff (1983). The simulations for axisymmetric dynamo action shown in the following are results from our 2D dynamo code MAGDISK with details given in Camenzind and Lesch (1990).

2. Observational Link between Accretion Disk and Bipolar Outflows

Accretion disks are present in various astrophysical systems: protostellar systems, cataclysmic variables, binary systems containing neutron stars and in the centers of active galaxies (Seyfert galaxies, Quasars and Radio Galaxies). A great fraction of these systems also show bipolar outflows with varying wind velocities and mass-loss. In this talk we discuss a completely general

scenario for the origin of accretion-driven outflows in protostellar systems and AGNs. It turns out in fact that protostellar systems and the centers of galaxies have many properties in common.

2.1 Protostellar Systems

There is now great evidence that low-mass YSOs ($M_* \leq 2$ $M_\odot$) are surrounded by circumstellar disks with masses $M_D \simeq 0.001 - 1.0$ $M_\odot$ on scales $\simeq 10^2 - 10^3$ AU (Beckwith et al., 1990). These disks extend in some systems even downward to the stellar surface (Bertout, 1989), but Beckwith et al. (1990) found in general an emission gap between the stellar surface and the inner edge of the disk. Observations on YSOs provide evidence for the simultaneous presence of accretion disks and energetic outflows in these sources and they point to a relationship between the outflows and the possible role of magnetic fields in disks and outflows (for many details see Königl, 1989). The relevant cornerstones of the observations can be summarized as follows (Appenzeller and Mundt, 1989; Bertout, 1989). YSOs are frequently found to drive energetic, bipolar outflows which sweep up the ambient gas into expanding shells. These sources also show collimated high-velocity ($v_j \simeq 200$ - 1000 km/s) ionized jets (see Mundt, 1988) with mass-loss rates of $10^{-7} - 10^{-10}$ $M_\odot$ yr^{-1}. There are also neutral winds present in these sources with higher mass-outflow rates, but with lower velocities, $v_w \simeq 10 - 50$ km s^{-1}. Since L_*/c, where L_* is the bolometric luminosity, is typically much smaller than the estimated momentum discharge in the wind, this indicates that the outflow is not driven by radiation pressure. There is also direct evidence for a link between circumstellar disks and energetic outflows in YSOs. Naked T Tauri stars (WTTS) are very similar to classical T Tauri stars (CTTSs) except they do not show any infrared excess and UV-excess, which are signatures for efficient accretion from some circumstellar disks. They also lack the strong low-ionization and forbidden emission lines as well as the P Cygni line profiles which are the indicator for energetic outflows (Appenzeller and Mundt, 1989). This simultaneous absence of evidence for inner disk accretion and strong winds in WTTSs points to a likely connection between inner disks and disk-winds. The properties of CTTSs suggest therefore that the outflows are powered by accretion. There is also evidence that this association between accretion disks and energetic outflows extends to higher luminosities as well (Strom, Strom and Edwards, 1988; Poetzel et al., 1989; Hessman et al., 1990). Circumstellar disks also affect the forbidden lines in T Tauri stars which often show a systematic blue shift (Appenzeller, 1989; Edwards et al., 1989). These line shifts are generally attributed to obscuration in the receding part of TT winds by the disk and therefore to a predominance of emission from the blueshifted part of the flow.

The energetic winds emanating from young stellar objects manifest themselves as high-velocity molecular flows, and in the form of strongly collimated optical jets (Lada, 1985; Fukui, 1989; Mundt et al., 1989). The mechanical luminosities in these flows are in the range of 0.002 - 0.1 of the luminosity L_* of the underlying star. The collimation of the molecular flows may occur within 0.02 pc of the central source. On the other hand, the optical jets are highly collimated (with opening angles of $5^0 - 10^0$) and appear to be collimated at radii ≤ 100 AU from the central star. Since the momentum flux exceeds L_*/c by factors of 100 - 1000, the flow is not driven by radiation pressure. Nowadays, the idea is generally adopted that magnetic forces are involved in the driving mechanism (Hartmann and McGregor, 1982; Draine, 1983; Pudritz and Norman, 1986; Shu et al., 1988). These magnetic fields themselves can provide also collimation of the flow (Blandford and Payne, 1982).

That these outflows originate from magnetic effects in disks follows from various observational facts. Polarization measurements revealed that the axis of the optical jets as well as of the swept-up molecular lobes are aligned within $\simeq 30^o$ of the ambient field direction for bipolar outflow sources (Appenzeller, 1989). This suggests that the magnetic field of molecular clouds influences the orientation of the circumstellar disks. These fields can therefore not be neglected in the accretion process, since differential rotation and advection will restructure and amplify the seed fields.

2.2 Accretion Disks in AGN

Direct evidence for the existence of accretion disks in AGN follows from the presence of a strong optical-UVX excess in the continuum of these sources (the so-called "Big Blue Bump", Malkan, 1989; Sun and Malkan, 1989; Ulrich, 1989). This bump cannot be fitted in terms of a single temperature blackbody (Laor and Netzer, 1989). The innermost part of these disks is somewhat hotter than the temperature expected from the boundary layer in the protostellar systems, $T_{\max} \simeq 30'000 - 100'000$ K. Since the temperature of standard disks scales as $T_D(R) \propto R^{-3/4}$, the temperature of disks in AGN also drops below the ionization limit for about 100 inner radii. The outer parts of the disks in AGN are then also relatively cool and consist of dusty matter similar to the disks in protostellar systems (Fig. 1).

Antonucci and Miller (1985) demonstrated that a torus of obscuring material completely hides a type 1 Seyfert nucleus from direct view in the case of the type 2 Seyfert NGC 1068. This model has been confirmed recently by X-ray observations (Elvis and Lawrence, 1988; Koyama, 1989). The torus of NGC 1068 is thick enough to block the $2 - 10$ keV X-rays from direct view, implying an absorbing column density of 10^{25} atoms cm^{-2}. These central condensations of molecular gas are considered to be the source of accretion

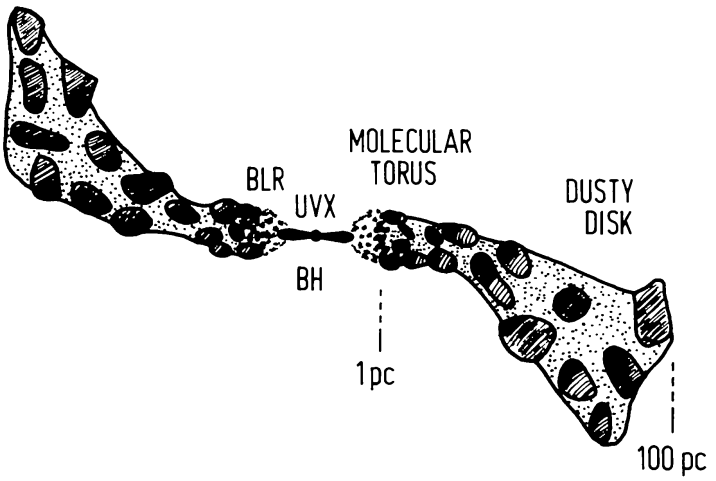

Fig. 1. Schematic view of the disk in AGN. The hot inner disk around a supermassive black hole (BH) produces the "big blue bump" (UVX), the broad emission line clouds (BLR) originate from the cooler middle part of the disk, and the infrared bump of radio-quiet objects may be emitted by dust in the outer part of the molecular torus. This molecular gas is also the fuel for the inner accretion disk.

fuel for the nucleus or for starburst activity (Fig. 1). It is still unclear how this gas is assembled on the parsec-scale from the much larger kiloparsec-scale (Krolik and Begelman, 1988). In this model, the classification of Seyfert types is determined by the angle of the line of sight to the torus: type 1 Seyferts are those viewed face-on, type 2 Seyferts are those viewed edge-on. A similar classification should hold for radio-weak quasars (Kawara et al., 1990). Barthel (1989) has also proposed that the distinction between radio galaxies and radio-loud quasars is based on the angle of the line of sight to the torus: quasars are those sources seen face-on, radio-galaxies are those viewed edge-on. In the torus models of Krolik and Begelman (1988) and Sanders et al. (1989), molecular clouds are destroyed at $\simeq$ 1 pc from the center, where the grains evaporate, producing in this way the famous 3.5 μm bump (the evaporation temperature of silicate grains is $\simeq$ 1500 K). When the dust sublimates, the molecular gas loses its primary opacity and cooling agent, the temperature rises above $\simeq$ 3000 K, and most molecules are destroyed. The observed H_2 emission of type 1 Seyferts and Quasars (Kawara et al., 1990) would come from the inner region of the molecular torus, while CO emission has its origin in the outer parts of molecular gas concentrations. The infrared bump of radio-quiet objects is then the result of dust emission from the outer parts of the disk (Sanders et al., 1989). Part of the infrared bump could however be due to non-thermal emission from magnetized coronae around the inner accretion disk (see later on). The angular sizes of these two emission regions differ by a factor of $\geq 10^4$.

Apart from the continuum emission of the disks in AGN, there is also direct kinematic evidence for rotation in a few objects. These objects show the classical double-peaked, broad emission lines which are considered to

be characteristic for Keplerian rotation. The prime candidates are 3C 390.3 (Oke, 1987; Perez et al., 1988) and Arp 102B (Halpern and Filippenko, 1988; Chen et al., 1989). Double-peaked difference spectra were also found in the Seyfert galaxy Akn 120 (Alloin et al., 1988) and in NGC 5548 (Stirpe et al., 1988). Standard thin disks do, however, not release sufficient gravitational energy locally at the radii where the Keplerian velocity corresponds to the observed width of the emission lines (typically at $\simeq$ 1000 Schwarzschild radii). Some extra source of energy is therefore needed (Collin-Souffrin, 1987).

Similar to protostellar systems, a subclass of AGN shows extremely energetic outflows extending even to scales beyond the outer edge of the galaxy in the form of strongly collimated radio jets (Bridle and Perley, 1984; Perley, 1989). The luminosities of these objects is an appreciable fraction of the luminosity of the underlying central object, and the flow speeds in these jets is at least semi-relativistic with a preponderance of extremely relativistic flows in superluminal sources, $\gamma_{\rm jet} \geq 2 - 20$ (Porcas, 1988; Zensus, 1989). As shown by VLBI observations, the collimation of these jets must occur on scales in general less than a fraction of a light year from the central source. It is generally accepted that magnetic forces are involved in the driving mechanism (Blandford and Payne, 1982; Blandford, 1989; Camenzind, 1986a, 1988, 1989b), and that the magnetic fields will also provide the collimation of the flow, since huge currents are in general involved in the jet flows (Benford, 1978, 1987; Camenzind, 1987b, 1989b; Heyvaerts and Norman, 1989; Lesch et al., 1989).

Magnetic fields are therefore very important for the understanding of the origin of bipolar outflows from disk-systems. Concerning the structure of these magnetic fields, there are two main questions. First, we would like to understand the origin of the fields in accretion disks and to find out the difference between sources with strong jets (such as Quasars) and sources with weak jets (QSOs and Seyfert galaxies). Secondly, once we know the structure of the magnetic fields in the disk, we have to elaborate the structure of the winds driven by these magnetic fields and to understand the collimation and acceleration mechanism.

3. The Origin of Magnetic Fields in Accretion Disks

The interstellar matter which accretes onto protostellar objects and supermassive objects in the centers of galaxies carries along magnetic fields. The evolution and influence of these magnetic fields on the structure of the disk are completely neglected in the theory of standard accretion disks. The evolution of magnetic fields in the disk depends on the nature of the electrical

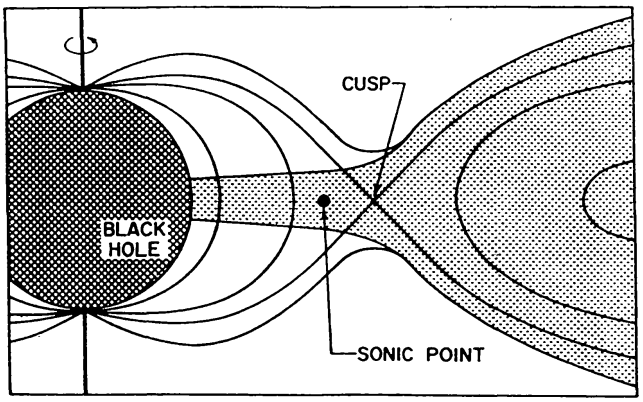

Fig. 2. A meridional cross-section through the boundary layer of a rotating black hole. The equipotential surfaces around a Kerr black hole show a cusp-like structure near the marginal stable orbit. The self-crossing surface forms a kind of Roche lobe. If the accretion disk overflows this Roche lobe, matter is accreted onto the horizon supersonically (Abramowicz and Zurek, 1981). The frame-dragging effect requires the plasma to corotate with the black hole near the horizon.

conductivity in the disk. At high temperatures Ohmic resistivity dominates in the disk, while in weakly ionized molecular gas ambipolar diffusion is an important process (the drift of ions and electrons, to which the magnetic field is frozen, relative to the neutrals in a weakly ionized medium). In a fully turbulent disk, the effective conductivity is however much lower due to turbulent processes.

3.1 Boundary Layers

Consider a steady accretion disk with accretion rate $\dot{M}$ around a central object of mass M and radius R_*. Throughout most of the disk the angular velocity of the disk material is Keplerian, $\Omega = \Omega_K(R)$. Between the central object and the disk we find in general a boundary layer (BL), in which the angular velocity varies between $\Omega_K(R_*)$ and Ω_*. For a black hole, $\Omega_* = \Omega_H$ is the angular velocity of the black hole ($\Omega_H = 0$ for a Schwarzschild black hole, $\Omega_H = a/(r_H^2 + a^2)$ for a Kerr black hole with angular momentum a). In purely hydrodynamical models, the width ΔR of the BL is small, $\Delta R \simeq H^2/R$, when H is the disk-thickness (Kley, 1989). For rotating black holes, this width is much broader, extending to a few Schwarzschild radii (Fig. 2), since there are no stable Keplerian orbits between the horizon and the marginally stable orbit (Breuer, 1975). Relativity, however, requires the accreting plasma to corotate with the black hole near the horizon, quite similar to accretion onto a non-collapsed object. The only difference is that the plasma flows supersonically through the horizon (Abramowicz and Zurek, 1981).

The energy generated in a Newtonian boundary layer is

$$L_{\rm BL} \simeq \frac{GM\dot{M}}{2R_*}\left(1-\frac{\Omega_*}{\Omega_K}\right)^2 \tag{1}$$

with $L_{\rm BL} \simeq L_D$ for the disk-luminosity when $\Omega_* \ll \Omega_K(R_*)$,

$$L_D \simeq \frac{GM\dot{M}}{2R_*}\,. \tag{2}$$

This is half of the available accretion luminosity $L_{\rm acc}$

$$L_{\rm acc} = \frac{GM\dot{M}}{R_*}\,. \tag{3}$$

The boundary layer around black holes must be treated relativistically. This is a completely unsolved problem.

The discussion of BLs must be based on some assumption about the viscosity. The standard picture of viscosity in disks relies on some kind of turbulent viscosity with turbulent eddies of maximal size $L_T \simeq H$ and turbulent speeds $v_T \leq c_S$, where c_S is the local sound speed. This gives rise to the Shakura and Sunyaev (1973) α-parametrization for the kinematic viscosity

$$\nu_T \simeq \alpha\, c_S\, H \simeq \alpha\, \Omega\, H^2(R) \quad , \quad \alpha = \frac{L_T}{H}\,\frac{v_T}{c_S} \leq 1\,. \tag{4}$$

In the boundary layer itself the length scales become typically smaller. Here one needs some formula for ν_T which takes the reduced length scales into account (Tylenda, 1981). The α-formula also applies for magneto-hydrodynamic turbulence, $v_A \leq c_S$, when $v_A = \sqrt{B^2/4\pi\rho}$ is the Alfvén speed in the disk.

3.2 Axisymmetric Dynamos in Disks

Fully turbulent disks are ideal set-ups for magnetic dynamos, quite similar to the dynamo action in the disks of spiral galaxies (Parker, 1971; Ruzmaikin et al., 1988; Krause et al., 1990). The essential ingredients for $\alpha\Omega$-dynamos are strong shear plus a density gradient perpendicular to the shear. Any small seed field which is initially present will decay exponentially or will be amplified by the dynamo until it reaches a maximum value with $v_A \simeq c_S$, i.e. $\alpha \simeq 1$. This would indicate that the magnetic contribution to the viscosity is dominant.

In turbulent disks, the magnetic fields evolve according to the induction equation of mean field electrodynamics (Moffatt, 1978; Krause and Rädler, 1980; Pudritz, 1981)

$$\partial_t \boldsymbol{B} + (\boldsymbol{u}\cdot\nabla)\,\boldsymbol{B} = (\boldsymbol{B}\cdot\nabla)\boldsymbol{u} - (\nabla\cdot\boldsymbol{u})\,\boldsymbol{B} + \nabla\wedge\left\{\mathcal{E} - \eta_T\,\nabla\wedge\boldsymbol{B}\right\}. \tag{5}$$

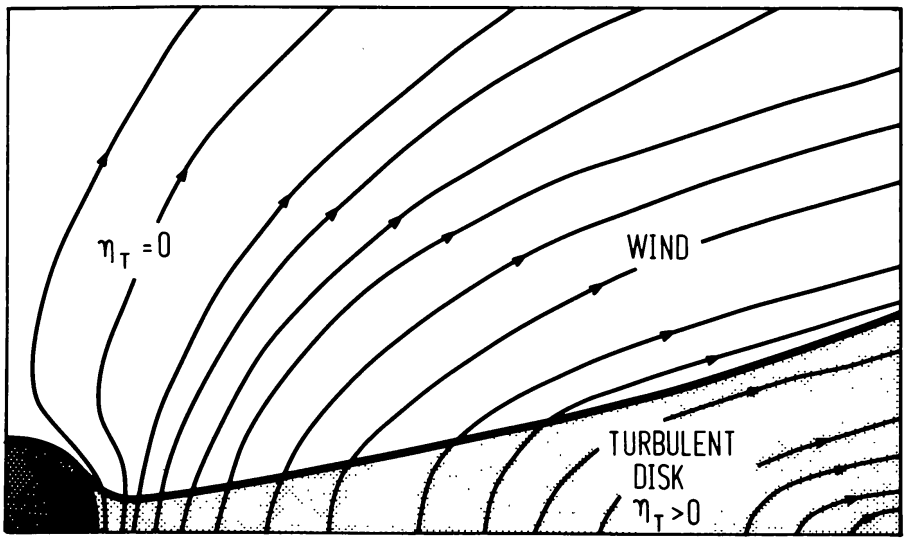

Fig. 3. The general set-up of a fully turbulent accretion disk around some collapsed or non-collapsed object. Strong differential rotation and turbulence in the disk will generate large-scale magnetic fields which build up a rotating magnetosphere around the disk. Plasma from the disk can flow into this magnetosphere and initiate strong outflows.

$\boldsymbol{B}$ is the mean magnetic field, and $\boldsymbol{u}$ the mean velocity field in the disk, $\boldsymbol{u} = (u_R, R\Omega, 0)$. η_T is the total magnetic diffusivity including the microscopic one and the turbulent diffusivity. $\mathcal{E} = \alpha_D \mathbf{B}$ represents the electromotive force induced by correlations between turbulent motions and turbulent magnetic fields. For axisymmetric fields, the above equation can be written as a coupled system for the poloidal magnetic flux $\Psi(t, R, z)$ and the poloidal current flux $T(t, R, z) = R B_\phi(t, R, z)$ (Camenzind, 1990b)

$$B_R = -\frac{1}{R}\frac{\partial \Psi}{\partial z} \quad , \quad B_z = \frac{1}{R}\frac{\partial \Psi}{\partial R}, \tag{6}$$

$$\frac{\partial \Psi}{\partial t} + u_R \frac{\partial \Psi}{\partial R} - \eta_T R^2 \nabla \cdot \left\{ \frac{1}{R^2} \nabla \Psi \right\} = \alpha_D T, \tag{7}$$

$$\frac{\partial T}{\partial t} + u_R \frac{\partial T}{\partial R} - R^2 \nabla \cdot \left\{ \frac{\eta_T}{R^2} \nabla T \right\} + T \frac{R\,\partial (u_R/R)}{\partial R} = R^2 \mathbf{B}_p \cdot \nabla \Omega + R^2 \nabla \cdot \left\{ \frac{\alpha_D}{R^2} \nabla \Psi \right\}. \tag{8}$$

These equations show the redistribution of the fluxes Ψ and T over the effect of spatial diffusion and radial advection. The shear $R\nabla\Omega$ will convert the poloidal field into a toroidal one. The fluxes Ψ and T are regenerated by helicity $\alpha_D(R, z)$ in the turbulent fluid (Ruzmaikin et al., 1988; Rüdiger, 1990)

$$\alpha_D = L_T^2 \, \Omega \, \bar{\alpha}(z)/H(R). \tag{9}$$

Since differential rotation is extremely strong in boundary layers, where the rotation is adjusted to the rotation of the central object, we expect strong amplification of magnetic fields in such boundary layers. Then also the Parker instability occurs which allows flux to escape from the disk and reconnection to take place. If viscosity is of magnetic origin, the free shear energy in the disk is converted into magnetic energy at the rate (per unit disk area)

$$Q^+ \simeq \nu_T \, \Sigma \, (R\Omega')^2 \simeq \frac{B^2}{8\pi} v_A \quad , \quad v_A \simeq \alpha H \Omega \, . \tag{10}$$

In equilibrium, this flux must be destroyed or removed from the disk in a kind of magnetized wind.

The solutions of the dynamo equations are in general not stationary. For this reason, we developed the time-dependent simulation code MAGDISK, based on finite elements, for the solution of the coupled system (7) and (8) (Camenzind, 1990b; Camenzind and Lesch, 1990) and for given structure functions $\eta_T(R,z)$, $\Omega(R,z)$, $\alpha_D(R,z)$ and $u_R(R)$. When the dynamo equations are normalized for the inner edge of the accretion disk ($R \to R/R_{\rm in}$, $z \to z/R_{\rm in}$, $t \to t/t_D$, $t_D = R_{\rm in}^2/\eta_{T,{\rm in}}$, $u_R = -u_{\rm in}\, u(R/R_{\rm in})$, $\alpha_D = \alpha_{D,{\rm in}}\, \bar{\alpha}_D$)

$$\frac{\partial \Psi}{\partial t} - R_m \, u \, \frac{\partial \Psi}{\partial R} - \bar{\eta}_T \, R^2 \nabla \cdot \left\{ \frac{1}{R^2} \nabla \Psi \right\} = R_\alpha \, \bar{\alpha}_D \, T \, , \tag{11}$$

$$\frac{\partial T}{\partial t} - R_m \, u \, \frac{\partial T}{\partial R} - R^2 \, \nabla \cdot \left\{ \frac{\bar{\eta}_T}{R^2} \nabla T \right\} - R_m \, T \, \frac{R \partial (u/R)}{\partial R} = R_\Omega \, R^2 \, \mathbf{B}_p \cdot \nabla \bar{\Omega} + R_\alpha \, R^2 \, \nabla \cdot \left\{ \frac{\bar{\alpha}_D}{R^2} \nabla \Psi \right\} , \tag{12}$$

the strength of the various terms in these dynamo equations are measured by means of the corresponding dynamo numbers

$$R_\Omega = \frac{R_{\rm in}^2 \, \Omega_{\rm in}}{\eta_{T,{\rm in}}} = \frac{R^2 \Omega}{\alpha \, P_m H^2(R) \Omega} = \frac{1}{\alpha P_m} \left(\frac{H_{\rm in}}{R_{\rm in}} \right)^{-2} , \tag{13}$$

$$R_\alpha = \frac{R_{\rm in} \, \alpha_{D,{\rm in}}}{\eta_{T,{\rm in}}} = R_\Omega \left(\frac{H_{\rm in}}{R_{\rm in}} \right) \left(\frac{L_T}{H_{\rm in}} \right)^2 , \tag{14}$$

$$R_m = \frac{R_{\rm in} \, u_{R,{\rm in}}}{\eta_{T,{\rm in}}} = \frac{1}{P_m} = \alpha \, R_\Omega \left(\frac{H_{\rm in}}{R_{\rm in}} \right)^2 . \tag{15}$$

α is the parameter of standard accretion disks (Eq. (4)) and P_m the magnetic Prandtl number, $\eta_T = P_m \, \nu_T$, $P_m \simeq 1$. For geometrically thin accretion disks, the dynamo numbers have the following relations (characteristic for $\alpha\Omega$-dynamos)

$$R_m < R_\alpha < R_\Omega \, . \tag{16}$$

In geometrically thick disks, differential rotation and helicity would be of the same order of magnitude, $R_\Omega \simeq R_\alpha \simeq R_m/\alpha$ ($\alpha^2\Omega$-dynamos).

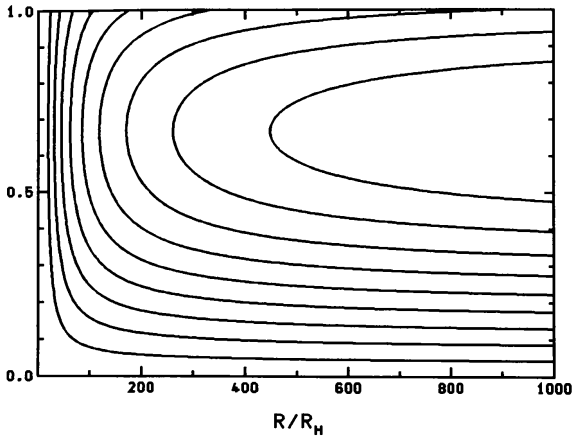

Fig. 4a. Poloidal field lines for stationary solutions in geometrically thin accretion disks without dynamo effect, $R_\alpha = 0$, $R_\Omega = 600$, $R_m = 200$, R_H: horizon radius, $\zeta = z/H$ (Khanna and Camenzind, 1990).

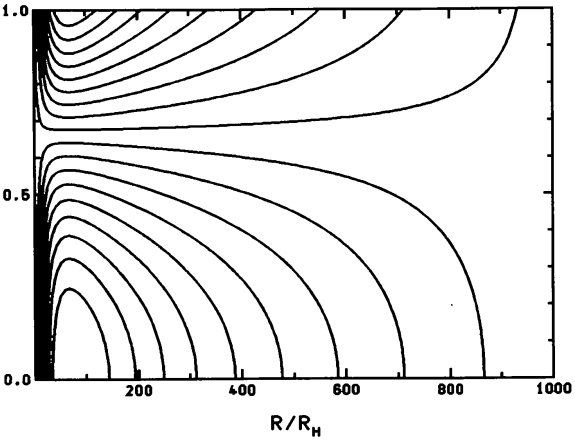

Fig. 4b. The distribution of the poloidal currents for the solutions, $RB_\phi = const$ (in units of Gauss cm).

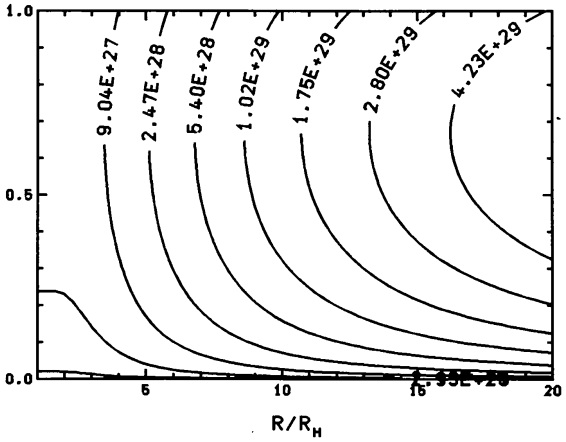

Fig. 4c. Inner part of the poloidal field structure shown in Fig. 4a (Ψ in units of Gauss cm^2).

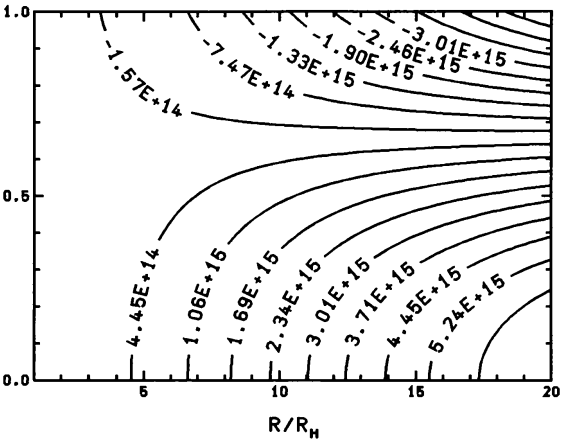

Fig. 4d. The inner part of the poloidal current structure of Fig. 4b (RB_ϕ in units of Gauss cm).

3.3 Stationary Solutions

When the α-effect is neglected in a disk, $\alpha_D = 0$ throughout the disk, the strong differential rotation amplifies the toroidal field. The poloidal flux Ψ is however only redistributed in the disk by advection and diffusion (there is no source term for Ψ). In this case, stationary solutions are generic and have been discussed by Lovelace et al. (1987) and Königl (1989). In Fig. 4 we

show solutions for $R_\alpha = 0$ in the thin disk approximation for a R-dependent magnetic diffusivity $\eta_T(R)$ around supermassive black holes (Khanna and Camenzind, 1990). In this case, accretion from the molecular torus advects a total magnetic flux $\Psi_\infty (= 5.7 \times 10^{30}$ Gauss cm^2) inwards and builds up a global quadrupolar field geometry which can also close to the horizon (Fig. 4c). The negative radial magnetic field near the equatorial plane produces there a positive toroidal field (Fig. 4b), and the positive radial magnetic field in the upper part of the disk is converted into a negative toroidal field (Fig. 4d). The maximum of B_ϕ occures near 30 R_H. The total current driven by differential rotation is $\simeq 10^{17}$ Ampère corresponding to a maximal toroidal field of $\simeq 10$ Gauss.

This example of a thin disk solution of the stationary dynamo equations shows that the magnetic field has not a self-similar structure (as assumed a priori e.g. by Königl (1989)). It also demonstrates that advection and diffusion alone cannot produce a flux distribution which is highly peaked near the inner edge of the disk (compare with the true dynamo solution in Fig. 6). For $R_\alpha = 0$, one can also construct similar solutions for dipolar configurations.

3.4 Disk-Corona Systems

The stationary solutions discussed in the previous section are in general not stable against the inclusion of the dynamo effect (i.e. for a non-vanishing α_D). From the experience with spherical dynamos we know that in systems with strong differential rotation ($R_\Omega \gg R_\alpha$) axisymmetric quadrupole modes have the highest probability to be excited, while for $\alpha^2\Omega$-dynamos also axisymmetric dipolar modes can grow (Brandenburg et al., 1990). In geometrically thin disks we expect therefore that dipolar modes would decay, but quadrupolar modes to grow under certain conditions (Brandenburg et al., 1990). The behaviour of the disk dynamo depends essentially on the two dynamo numbers R_Ω and R_α (Fig. 5). For each value of R_Ω we find a corresponding critical value for R_α, where the system is stationary. For values of R_α higher than this critical value, the magnetic fields grow exponentially, but they would decay exponentially for values smaller than the critical one. The solid line in Fig. 5 represents this critical curve for axisymmetric quadrupolar modes, the dahsed line for dipolar modes. The exact shape of this critical line is not yet known for accretion disks.

Using our time-dependent solver MAGDISK for the system (11) and (12) (Camenzind and Lesch, 1990), we found one critical point for $\alpha P_m = 1/3$ and $H_{\rm in}/R_{\rm in} = 0.1$ ($R_\Omega = 300$, $R_\alpha = 30$ and $R_m = 3$) which is denoted as a star in Fig. 5. Since for disks, $R_\alpha = \sqrt{R_\Omega/\alpha P_m}$, disk models with fixed values of αP_m would move along the thin solid lines in Fig. 5, when $H_{\rm in}$ is varied. Large scale magnetic fields would not exist in the region below the critical line.

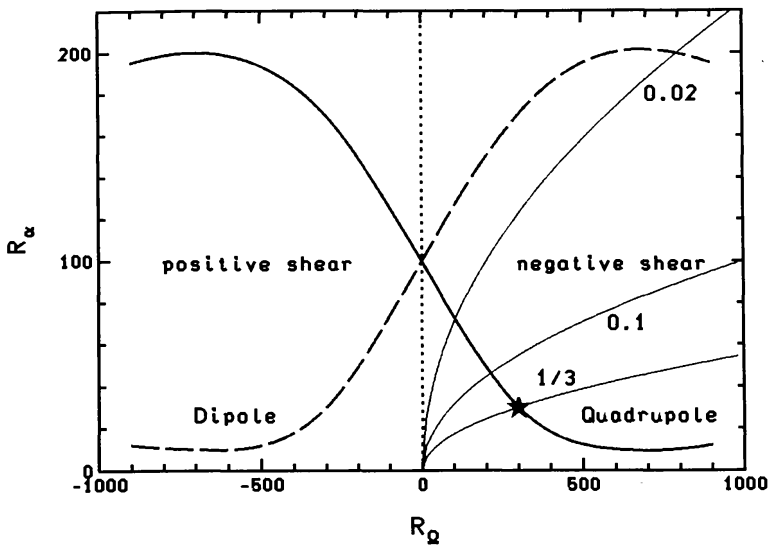

Fig. 5. The dynamo number plane (R_Ω, R_α) for axisymmetric modes in accretion disks. $R_\Omega > 0$ means a negative shear, $R\partial_R\Omega < 0$. Axisymmetric modes can only grow above the solid line for the corresponding mode. The exact critical dynamo numbers are not yet known for turbulent accretion disks. The star marks one point we found in our simulations. Quadrupolar modes grow exponentially above the solid line, dipolar modes above the dashed line. Accretion disks move along the thin solid lines for given αP_m, when the disk height H is varied.

In Fig. 6 we show the solutions of the dynamo equations for a disk-corona system, where the turbulent diffusivity η_T vanishes in the corona. For $R_\Omega = 300$, $R_\alpha = 30$ and $R_m = 3$, the quadrupolar field is marginally stationary and grows exponentially for higher dynamo numbers (Fig. 5), but would decay exponentially for much lower dynamo numbers. Differential rotation in the corona also excites a positive toroidal field there which grows to the same strength as the negative toroidal field in the disk itself. We find that the global behaviour of the magnetic fields depends largely on the z-dependence of η_T, quite similar to the behaviour we found for galactic dynamos (Camenzind and Lesch, 1990).

For supercritical dynamo numbers, seed fields in the disk are rapidly amplified and grow in general exponentially, until equipartition with the turbulence is reached. Realistic solutions of the dynamo equations must include therefore the feedback of the magnetic fields on the evolution of the turbulence in the disk and corona and the feedback on rotation and radial motion (Heyvaerts and Priest, 1989). A configuration with $B_\phi \gg B_p$ is in general unstable to magnetic buoyancy. The entire azimuthal flux tube is lifted up above the disk and now forms a low-β hot corona ($\beta = P_g/P_m$) (see also Shibata et al., 1989; Matsumoto et al., 1990). This interaction between the disk-corona and the disk itself will saturate the exponential growth of the disk-fields. For extremely high dynamo numbers, more complicated magnetic field distributions with various nodes can be excited. As shown by Eq. (13), this will occur for extremely thin disks or for low α-values.

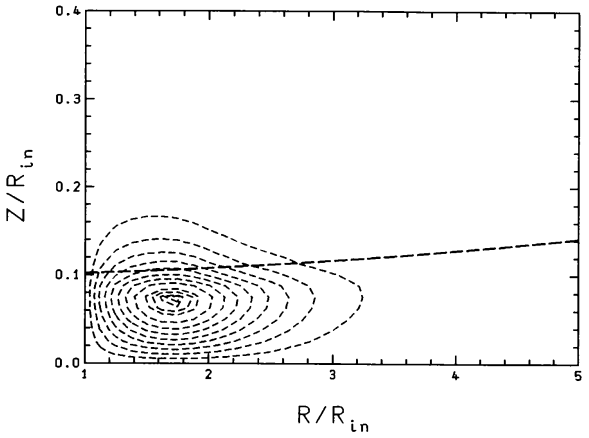

Fig. 6a. Poloidal field distribution in geometrically thin disks with parameters $\Omega_* = 0.8\Omega_K(R_*)$ for the dynamo numbers $R_\Omega = 300$, $R_\alpha = 50$, $R_m = 3$, $t = 1.5t_D$, $H_{\rm in}/R_{\rm in} = 0.1$.

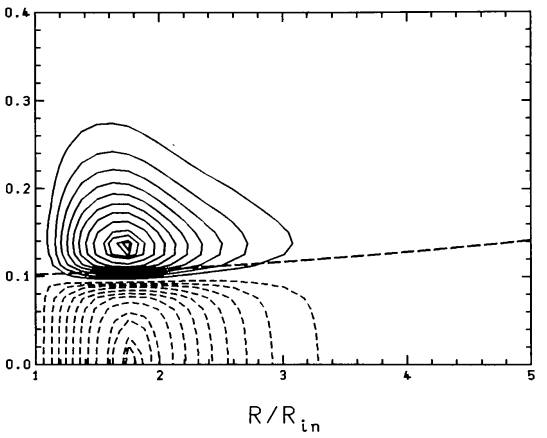

Fig. 6b. The toroidal field distribution for Fig. 6a. The dashed line marks the scale height of the disk as used in the simulation.

4. The Structure of Axisymmetric Magnetized Outflows

Dynamo action in the disk forms a rotating magnetosphere which will be deformed by outflowing corona plasma. The poloidal plasma flow must, therefore, be included in the description of the exterior solutions. Exterior to the disk the magnetic structure has to be modeled as a wind magnetosphere. The rapid rotation of inner disks in AGN forces us to use general relativistic MHD on a Kerr background (Camenzind, 1986a, b, 1987, 1989a, b; Haehnelt and Camenzind, 1990). The following treatment of the problem, however, neglects the influence of gravity. Since we are mainly interested in the equilibrium configurations for these wind magnetospheres, we can use a stationary approach. It is well known that in this case the plasma has to flow parallel to the magnetic field, i.e. the poloidal velocity $\mathbf{u}_p$ is proportional to the poloidal magnetic field $\mathbf{B}_p$

$$\mathbf{u}_p = \frac{\eta}{n}\mathbf{B}_p \quad , \quad u^\phi = \left(\frac{\eta}{n}B_\phi + R\,\Omega^F\right) . \tag{17}$$

n is the particle density in the flow and η is constant along the magnetic flow lines ($\mathbf{B}\cdot\nabla\eta = 0$). This relation means that we know the flow direction, once we know the structure of the magnetosphere. With these quantities we define the special relativistic Mach number M (Camenzind, 1986a)

$$M^2 = \frac{4\pi\mu\, n\, u_p^2}{B_p^2} \quad , \quad \mu = \frac{\rho + P}{n} \simeq m_p c^2 , \tag{18}$$

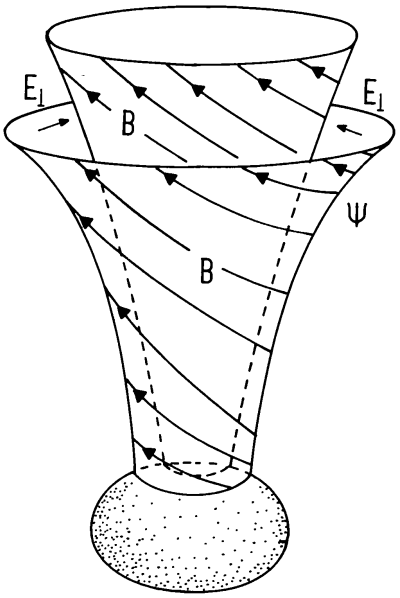

Fig. 7. The structure of relativistic magnetized winds. The wind ejected by rotating objects consists of a nested family of magnetic surfaces. Due to the rotation, toroidal fields are also produced. This rotation of the field lines provides an electric field perpendicular to the magnetic surfaces. The wind plasma is flowing along these magnetic surfaces

which tells us, whether the flow is strongly magnetized ($M^2 \ll 1$) or weakly magnetized ($M^2 \geq 1$). For low velocities near the disk surface, the magnetic field controls the flow, but far away from the disk the flow becomes super-Alfvénic.

4.1 The Concept of Magnetic Surfaces

The essential ingredient for the global structure of axisymmetric hydromagnetic flows is the concept of magnetic surfaces. Due to axisymmetry, hydromagnetic flows consist of a family of nested magnetic surfaces $\Psi = const$, where the quantity $2\pi\Psi$ describes the magnetic flux enclosed by a cross section, which cuts the corresponding magnetic surface and the rotational axis (see Fig. 7). In the high conductivity limit, plasma is forced to flow along these surfaces, and these surfaces are also electric potential surfaces, i.e. the electric field $\mathbf{E}$ is orthogonal to the magnetic surface

$$\mathbf{E} = -\frac{R\Omega^F}{c}\,\mathbf{e}_\phi \wedge \mathbf{B}_p = -\frac{\Omega^F}{c}\,\nabla\Psi\,. \tag{19}$$

The magnetic surfaces have an additional property: they rotate with the angular frequency $\Omega^F(\Psi)$ which is constant along the surface, but varies from surface to surface. Its value is given by the rotation of the magnetic field at its foot point in the disk. This angular velocity defines a light cylinder radius for each field line, $R_L = c/\Omega^F$.

The magnetosphere also carries poloidal currents $\mathbf{j}_p$ which follow from the toroidal magnetic field B_ϕ

$$\mathbf{j}_p = \frac{c}{4\pi R} \nabla(RB_\phi) \wedge \mathbf{e}_\phi \,. \tag{20}$$

The toroidal field itself follows from conservation equations ($x = R/R_L$)

$$RB_\phi = -4\pi \frac{\eta(\Psi) E(\Psi)}{\Omega^F} \frac{x_A^2 - x^2}{1 - M^2 - x^2} \,, \tag{21}$$

where $E(\Psi)$ represents the total energy per particle carried along the wind

$$E(\Psi) = \mu\gamma - \frac{R\,\Omega^F\, B_\phi\, B_p}{4\pi\, n u_p} \,. \tag{22}$$

The first term is the total mass-energy (γ the Lorentz factor of the flow) and the second term represents the magnetic energy in the flow, which vanishes for non-rotating configurations. Similarly, $L(\Psi)$ is the total angular momentum carried in the wind

$$L(\Psi) = \frac{\mu}{c^2} \gamma\, R^2\, \Omega - \frac{R\, B_\phi\, B_p}{4\pi\, n u_p} \,. \tag{23}$$

From expression (21) for B_ϕ we see that the Alfvén point of the flow is in the relativistic case not at $M^2 = 1$ as in Newtonian MHD ($R = R_A$, $x = x_A$), but slightly changed by

$$M_A^2 = 1 - \Omega^F\, L(\Psi)/E(\Psi) \leq 1 \,. \tag{24}$$

When the flow is strongly magnetized, $M_A^2 \ll 1$ and therefore $\Omega^F L/E \to 1$, the Alfvén point moves towards the light cylinder, $R_A \to R_L$, and RB_ϕ is then only a function of the magnetic surface

$$RB_\phi = -\frac{2}{c} I(\Psi) = -4\pi \frac{\eta(\Psi)\, E(\Psi)}{\Omega^F} = -4\pi\, \eta(\Psi)\, L(\Psi) \,, \tag{25}$$

i.e. in this case the angular momentum distribution determines the current distribution $I(\Psi)$ in the magnetosphere. As a consequence, we find $\mathbf{j}_p \parallel \mathbf{B}_p$,

$$\mathbf{j}_p = -\frac{dI}{2\pi\, d\Psi} \mathbf{B}_p \,. \tag{26}$$

In summarizing, we find that magnetized coronae and winds consist of a nested family of magnetic surfaces, the plasma must flow along these surfaces and the poloidal currents also flow along the surfaces, when the flow is strongly magnetized. The next question is therefore to find out the form of these surfaces.

4.2 The Grad-Schlüter-Shafranov Equation (GSS)

One of the essential points of the computation of self-consistent MHD disk-winds is the particular form of the toroidal current j_ϕ, which determines the structure of the wind-magnetosphere via Ampère's equation

$$\nabla \wedge \mathbf{B}_p = \frac{4\pi}{c} j_\phi \mathbf{e}_T \quad , \quad \mathbf{B}_p = \frac{1}{R}(\nabla\Psi \wedge \mathbf{e}_T). \tag{27}$$

With the introduction of the magnetic flux function Ψ, which we now use as our stream function, this equation can be transformed into a divergence equation of the form

$$R\nabla \cdot \left\{ \frac{1}{R^2} \nabla\Psi \right\} = -\frac{4\pi}{c} j_\phi \,. \tag{28}$$

Plasma confinement in the laboratory and in solar filaments is based on this equation, known as the Grad-Schlüter-Shafranov (GSS) equation. When plasma is moving along the magnetic flux surfaces, the general form of the current j_ϕ follows from a force balance perpendicular to the flux surfaces. For this purpose one considers the relativistic Lorentz force

$$n(\mathbf{u}\cdot\nabla)(\mu\mathbf{u}) + \nabla P = \rho_e \mathbf{E} + \frac{1}{c}(\mathbf{j} \wedge \mathbf{B}). \tag{29}$$

The projection of this equation perpendicular to the magnetic flux surfaces provides then the current j_ϕ (a derivation is given in Camenzind, 1987a)

$$\begin{aligned}\frac{1}{c} B_p j_\phi (1 - M^2 - x^2) = &-\frac{RB_\phi}{4\pi R^2} \nabla_n (RB_\phi) + \rho_{GJ} E_n \\ &- \mu\gamma n\{\nabla_n \gamma - \Omega \nabla_n l\} - \nabla_n P + \mu\eta B_p^2 \nabla_n (\eta/n).\end{aligned} \tag{30}$$

$\mathbf{n}$ is the normal unit vector of the magnetic surfaces. In the *force-free limit*, where plasma inertia is neglected, $\nabla_n P = 0 = \nabla_n \gamma = \nabla_n l$, we obtain

$$B_p j_\phi (1 - x^2) = -c \frac{RB_\phi}{4\pi R^2} \nabla_n (RB_\phi) + c\rho_{GJ} E_n \,, \tag{31}$$

so that the current is given as (ρ_{GJ} is the Golreich-Julian density)

$$j_\phi (1 - x^2) = 4c \frac{I(\Psi)}{4\pi R} I'(\Psi) + c\rho_{GJ} \frac{E_n}{B_p} \,. \tag{32}$$

It is then easy to show that the GSS-equation (28) can be written in the suggestive form of

$$R\nabla \cdot \left\{ \frac{1 - x^2}{R^2} \nabla\Psi \right\} = -\frac{4}{R} I I' \,, \tag{33}$$

which is the *classical pulsar equation* originally derived by Scharlemann and Wagoner (1973). This equation shows that the poloidal current distribution $I(\Psi)$ also determines the effective source for the poloidal fields.

The general GSS equation is a highly non-linear equation, since all the source terms have a complicated dependence on Ψ itself. In particular, $I(0) = 0 = I(\Psi_{\rm disk})$, when the total current flowing in the magnetosphere vanishes. Let us normalize the coordinates in units of light cylinder radii, the flux Ψ in units of the total flux Ψ_D produced by the disk, and the current in terms of its maximal value, $I = I_{\rm max}\bar{I}$. Then the general GSS equation including inertia effects can be written in a dimensionless form

$$x\nabla\cdot\left\{\frac{1-M^2-x^2}{x^2}\nabla\Psi\right\}+\frac{g_I}{x}\bar{I}\bar{I}'=-\frac{1}{\sigma_0^2}\bar{j}^{\rm inert}\,, \tag{34}$$

where the quantity

$$\sigma_0=\frac{\Psi_D}{4\pi\eta_0 mcR_L^2}\simeq\frac{\Psi_D^2}{2\dot{N}_{\rm wind}\,mc\,R_L^2} \tag{35}$$

acts as the inverse of a coupling constant for the inertial current $\bar{j}^{\rm inert}$. The source function $\bar{j}^{\rm inert}$ contains all contributions to the toroidal current density j_ϕ due to pressure and inertial effects in the force-balance equation (30). g_I is the coupling constant for the effects of the poloidal currents

$$g_I=\frac{4I_{\rm max}^2R_L^2}{c^2\Psi_D^2}\simeq 0.04\left(\frac{I_{\rm max}}{10^{18}\ {\rm Amp}}\right)^2\left(\frac{R_L}{10^{15}\ {\rm cm}}\right)^2\left(\frac{\Psi_D}{10^{33}\ {\rm G\,cm^2}}\right)^{-2}. \tag{36}$$

When the plasma density is small in the magnetosphere, we find $\sigma_0\to\infty$, $M^2\to 0$. In this case, the current distribution $I(\Psi)$ alone determines the form of the magnetic surfaces. This limit holds for AGN ($M > 10^8\ {\rm M}_\odot$), where

$$\sigma_0^{\rm AGN}\simeq 10\,\Psi_{D,33}^2\,\dot{M}_{w,-1}^{-1}\,R_{L,15}^{-2}\,, \tag{37}$$

for a mass flux $\dot{M}_{\rm wind}\simeq 0.1\ {\rm M}_\odot/{\rm yr}$ in the wind and a disk magnetic flux $\Psi_D\simeq 10^{33}$ Gauss cm^2. This term is, however, dominant for stellar winds

$$\sigma_0^*\simeq 10^{-11}\,\Psi_{D,25}^2\,\dot{M}_{w,-8}^{-1}\,R_{L,15}^{-2}\,. \tag{38}$$

The computation of wind magnetospheres for AGN can therefore be handled in the force-free limit (33), while those for proto-stellar winds must be done with the full GSS equation (34). In the past few years we developed methods to solve the force-free GSS equation (Camenzind, 1987a)

$$x\nabla\cdot\left\{\frac{1-x^2}{x^2}\nabla\Psi\right\}+\frac{g_I}{x}\bar{I}\bar{I}'=0\,, \tag{39}$$

including also the effects of the gravitational background of a rotating Kerr geometry (Haehnelt and Camenzind, 1990). Unfortunately, there is

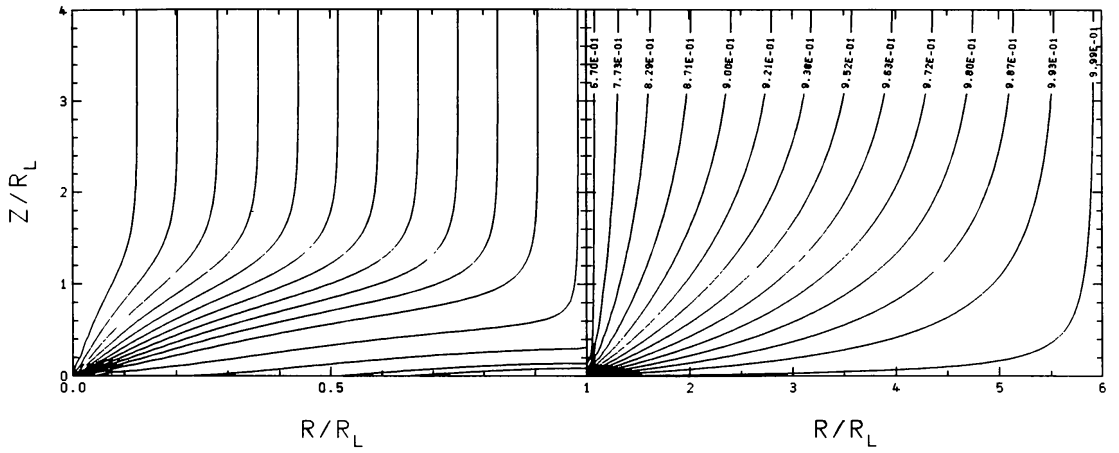

Fig. 8. The structure of the poloidal magnetic flux surfaces of a rotating magnetosphere produced by the accretion disk around a black hole. The outflow is collimated due to the strong pressure in galactic centers and the pinching force of the current-carrying magnetosphere.

not much known about analytic solutions of this equation, except for linear $I(\Psi)$ (Michel, 1982; Lovelace et al., 1987). We solved this equation by fixing the form of $\bar{I}(\Psi)$, and increasing slowly the coupling constant g_I. For low coupling constant, $g_I \ll 10^{-2}$, the magnetosphere has a universal form with field lines perpendicularly crossing the light cylinder (Figs. 8, 9). The solution exterior to the light cylinder is then completely determined by the flux distribution along the light cylinder and the boundary conditions at large distances. In the core of a galaxy, the escaping wind plasma will encounter a finite pressure $P_{\rm ext} \simeq 10^{-2}$ dyn cm^{-2}, which enforces pressure equilibrium of the wind with this ambient medium. The wind is therefore collimated in the direction of the rotational axis outside the light cylinder with a radius $R_{\rm jet}$ given by perpendicular pressure equilibrium (Fig. 8). The same holds for disk-winds in molecular clouds, but here the collimation already starts beyond the Alfvén radius $R_A \simeq 10\, R_{\rm in} \simeq 1$ AU (see Sec. 5.2).

4.3 Magnetized Winds

The terminal speed v_∞ of a cold MHD wind which flows along a given magnetic surface can readily been derived from the energy equation (see e.g. Michel, 1969)

$$v_\infty \simeq V_m = \left(\frac{\Omega_*^2\, \Psi_*^2}{\dot{M}_w}\right)^{1/3} = \left(\frac{\Psi_*^2\, c^2}{\dot{M}_w\, R_L^2}\right)^{1/3} . \qquad (40)$$

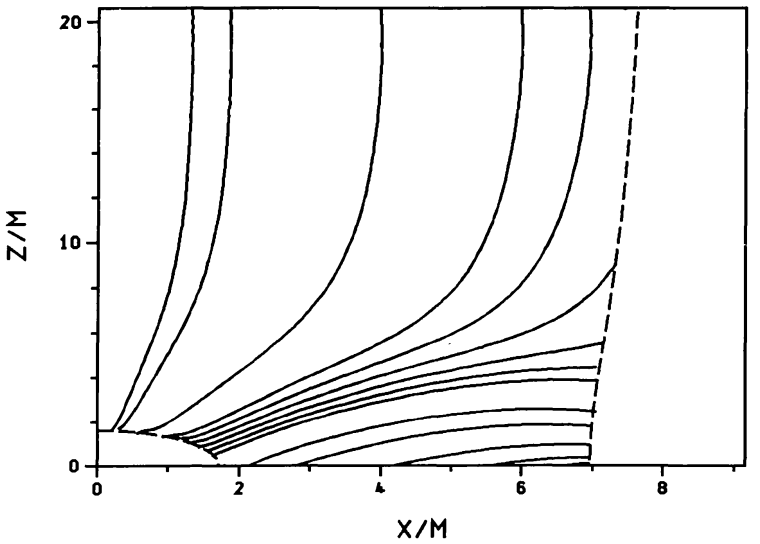

Fig. 9. Distribution of the dipolar poloidal flux around a rotating black hole with angular momentum $a = 0.8\, M_H$ (Haehnelt and Camenzind, 1990). This solution includes the gravitational effects of a rotating Kerr black hole. $M = GM_H/c^2$, the dashed lines denote the position of the inner and outer "light cylinder".

Ψ_* is the poloidal magnetic flux enclosed by the axisymmetric flux-tube at its foot point on the disk, $\dot{M}_w$ the mass-flux in the wind and R_L the corresponding light cylinder radius. In general, this relation will be scaled by some factor because the exact value of the terminal speed will depend on the particular form of the flux-tube.

In the relativistic case, the poloidal velocity of the plasma streaming along a given flux tube in the rotating magnetosphere follows from the normalisation of the 4-velocity, $u^\alpha u_\alpha = 1$. Since the Lorentz factor γ and the specific angular momentum l are determined by the conservation laws for the total energy and angular momentum, the solution of the poloidal velocity defined as $u_p^2 = -u^A u_A$ $(A = 1, 2)$ follows from the expressions discussed in the last section

$$u_p^2 + 1 = \gamma^2 \left(1 - l^2/R^2\right) . \tag{41}$$

The above equation for u_p is still implicit, since the Mach number M also contains the poloidal velocity. By using the definition of η, $\eta/n = u_p/B_p$, $B_p^2 = -B^A B_A$, $x = R/R_L$, we can, however, decompose this Mach number in a suitable way as

$$M^2 = 4\pi m \eta c^2 \, \frac{\mu}{mc^2} \, \frac{\eta}{n} = u_p \, x^2 \, \frac{\Phi(R)}{\sigma_*(\Psi)} , \tag{42}$$

with the following parameters

$$\Phi(R) = \frac{B_{p,D} R_D^2}{B_p R^2} , \tag{43}$$

$$\sigma_*(\Psi) = \frac{B_{D,\mathrm{in}} R_D^2}{4\pi\eta(\Psi) mc R_L^2} \simeq \sigma_0 \,. \tag{44}$$

With all these parameters, the above implicit equation for u_p can be transformed to a polynomial of degree 16 for a polytropic index $\Gamma = 5/3$, when the quantity $z_p = u_p^{1/3}$ is used instead of u_p (Camenzind and Endler, 1990)

$$\sum_{n=0}^{16} A_n\left(\frac{R}{R_L}, E, L, \frac{P_{\mathrm{in}}}{n_{\mathrm{in}} mc^2}; \frac{\Phi(R)}{\sigma_*}; g_{tt}, g_{t\phi}, g_{\phi\phi}\right) z_p^n = 0. \tag{45}$$

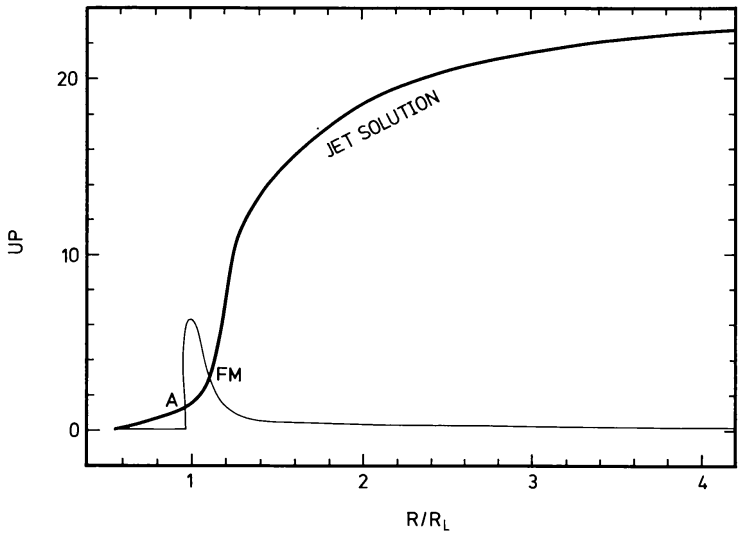

Fig. 10. The various solutions of the wind equation for a flux-tube of the accretion disk (Fig. 8). A: Alfvén point, FM: fast magnetosonic point, $u_p = \gamma v_p$.

The solutions of this hot wind equation depend on the initial parameters R_{in}, R_L, $B_{p,\mathrm{in}} R_{\mathrm{in}}^2$, $u_{p,\mathrm{in}}$, $P_{\mathrm{in}}/n_{\mathrm{in}} mc^2$, and the particle injection law $\eta(\Psi) = d\dot{N}/d\Psi$. Of central importance for the acceleration of the plasma is the form of the flux tube function Φ, defined by equation (43). Φ is constant for a monopole geometry, but has a complicated form for an open flux tube in the rapidly rotating magnetosphere. The equation for the poloidal velocity (or for the Lorentz factor) has two additional critical points, the slow and fast magnetosonic points. The parameters L and E are now constrained by the requirement that the physical wind solution passes through the Alfvén point and the fast magnetosonic point.

In Fig. 10 we show the various branches of solutions of the hot wind equation for a finite initial pressure in the background of a Kerr black hole with a flux tube given by the solution shown in Fig. 8. The injection of plasma occurs near the radius of maximum energy production in the disk. The physical wind solution starts with finite velocity near the slow magnetosonic point (near the injection point), crosses an unphysical branch at

the Alfvén point near the light cylinder and a second time at the fast magnetosonic point, and reaches finally a constant outflow velocity. Since the inertia of the plasma is included in our treatment, the light cylinder is no critical point of the wind equation. Without inclusion of gravity, the slow magnetosonic point does not appear in the solutions.

4.4 Energetics of Outflows

Magnetized disk winds carry in general two forms of energies, on the one hand kinetic energy from the acceleration and on the other hand also magnetic energy in form of the Poynting flux. The initial magnetic energy flow can be estimated from the expression for the Poynting flux $\mathbf{P}_p$, which follows from the expression for the total energy carried away, Eq. (22),

$$\mathbf{P}_p = \frac{c}{4\pi}\,(-B_\phi)\,\frac{R}{R_L}\,\mathbf{B}_p\,. \tag{46}$$

If we integrate this flux over the entire disk surface, we obtain the initial magnetic luminosity L_m of the flow

$$L_m \simeq \frac{c}{2}\,(-B_\phi)_D\,\frac{R_{\rm in}}{R_L}\,\Psi_{\rm disk} \simeq \frac{1}{c}\,\Omega^F\,I_{\rm max}\,\Psi_{\rm disk} \simeq I_{\rm max}\,\Psi_{\rm disk}/R_L\,. \tag{47}$$

For *protostellar objects* we get then

$$L_m \simeq 0.1\,L_\odot\,(-B_\phi)_D\,\Psi_{D,25}\,, \tag{48}$$

when the toroidal field in the disk is in units of Gauss and the total magnetic flux of the disk Ψ_D in units of 10^{25} Gauss cm^2. This magnetic luminosity will be partly transformed into kinetic energy of the outflowing wind, so that finally $L_w \leq L_m$. This estimate conforms nicely with the kinetic luminosities derived for the ionized jets in protostellar objects (Mundt et al., 1987). This magnetic luminosity has to be compared with the accretion luminosity $L_{\rm acc}$

$$L_{\rm acc} = \frac{1}{2}\,\dot{M}\,\frac{GM}{R_{\rm in}} \simeq 1.0\,L_\odot\,\dot{M}_{-7}\,\frac{3R_\odot}{R_{\rm in}}\,. \tag{49}$$

Similarly, we can estimate the magnetic luminosity of supermassive accretion disks in AGNs. Here we find toroidal fields typically of the order of a few kilo-Gauss and magnetic fluxes not exceeding 10^{34} Gauss cm^2. This corresponds to a total magnetic luminosity above the disk surface of

$$L_m \simeq 10^{47}\,{\rm erg\,s^{-1}}\,(-B_\phi)_{D,4}\,\Psi_{D,34}\,, \tag{50}$$

which is remarkably close to the accretion luminosity of strong Quasars.

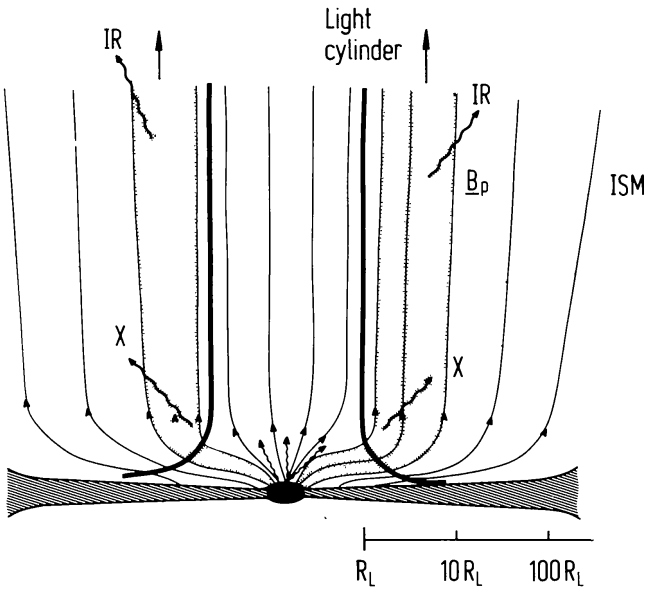

Fig. 11. The parsec-scale structure of magnetized jets in Quasars (Courvoisier and Camenzind, 1989). The central accretion disk carries a rotating magnetosphere which is strongly deformed by the presence of the light cylinder. The escaping disk-wind material is collimated outside the light cylinder by pinching forces. Stationary synchrotron emission (IR) occurs either near the light cylinder or the outer edge of the jet. The hot wind material can efficiently cool by Comptonization of the UV-flux from the inner disk and produce the hard X-ray emission (X).

5. Quasar and Protostellar Jets

The ionized winds emanating from the central boundary layers in AGN and protostars will be collimated on scales typically larger than the light cylinder radius of these objects. Disk-winds are therefore accelerated to disk-jets.

5.1 Quasar Jets

The parsec-scale jets of Quasars such as 3C 120 (Walker et al., 1987), 3C 273 (Cohen et al., 1987), or 3C 345 (Biretta et al., 1986) are visible in the synchrotron light in the GHz-range. At frequencies below 5 GHz, VLBI images of 3C 273 show a slightly curved jet which is 50 mas long (for z = 0.158 1 mas corresponds to 3.6 pc for H_0 = 50 km s^{-1} Mpc^{-1}) and has a complex brightness distribution. In this jet, superluminal components follow a common trajectory which is guided by the magnetic structure of the underlying relativistic plasma jet. With the higher resolution of millimeter-VLBI the motion of these superluminal knots can be traced even closer to the core (Krichbaum et al., 1990).

Relativistic jets in Quasars are formed in the rapidly rotating magnetosphere of accretion disks (Blandford and Payne, 1982; Lovelace et al.,

1987; Camenzind, 1986a, 1987b, 1988, 1989b). The accretion disk around a supermassive black hole creates a strong magnetosphere with typical field strengths of the order of a few kilo-Gauss at the surface of the disk (Figs. 9, 11). Normal plasma is then injected from the surface of the inner disk into this magnetosphere and is accelerated along the open magnetic flux tubes to final Lorentz factors $\gamma_{\rm jet} \simeq \sigma_* \simeq 10$, where σ_* is Michel's magnetization parameter defined in Eq. (44). If the flux tubes contain an extremely thin plasma, even higher Lorentz factors can be achieved. The collimation of the flux tubes towards the rotational axis of the disk occurs outside the light cylinder through the magnetic pinch effect and finite pressure effects in the center of a galaxy. The resulting jet radius is $\simeq (10-100)\ R_L$, and this inner region of the escaping jet is the origin of the self-absorbed synchrotron core emission (Krichbaum et al., 1990). The inner jet is also surrounded by a kind of magnetic cocoon formed through the interaction of the magnetized jet with the ambient hot interstellar matter. The expanding VLBI knots are then most probably the result of resistive instabilities which occur near the edge of the jet (for further discussion, see Courvoisier and Camenzind, 1989). The stability of these relativistic magnetized jets will depend on the total current carried along (Appl, 1990). There is also not much known about the propagation of these jets through the interstellar medium of a galaxy. Some numerical work has been done quite recently only on the propagation of non-relativistic magnetized jets (Kössl et al., 1990; Lind et al., 1989). Besides relativity, the essential unknown ingredient for such calculations is the finite resistivity of the magnetized jet material.

5.2 Protostellar Jets

We have argued that the most likely site of the origin of a hydromagnetic wind from an accreting protostar is the boundary layer between the inner accretion disk and the protostar (see also Pringle, 1989). Observationally, protostars are known to have rotation rates well below the break-up speed, $\Omega_*/\Omega_K \simeq 0.1$; the jet-source DG Tau has $v_* \sin i \simeq 22$ km s^{-1}, while $v_K(R_* \simeq 3R_\odot) \simeq 260$ km s^{-1}, i.e. $\omega = \Omega_*/\Omega_K(R_*) \simeq 1/5$ (Hartmann and Stauffer, 1989). This indicates that despite the high mass accretion rate the star has not been spun up to break-up rotation.

In the following we discuss a new model for the origin of the winds, the ionized jets and the low rotation rates observed in young stellar objects (Montmerle and André, 1988; Camenzind, 1990c). The essential assumption relies on the existence of a magnetized protostar (with fields of the order of a few hundred Gauss) and the existence of cool disks on the scale from 0.03 AU to ≥ 100 AU. This is the range of a few stellar radii to thousands of stellar radii. Provided the central protostar carries a magnetosphere with a more or less dipolar structure, there will be an equilibrium surface between this magnetosphere and the accretion disk, determined by pressure balance.

The pressure in a standard accretion disk follows from the expression (see e.g. Straumann, 1986)

$$P(R) = \frac{1}{I_{N+1}} \frac{\dot{M}}{4\pi\,\alpha\,R^2} \left(\frac{GM_*}{R}\right)^{1/2} \left(\frac{H}{R}\right)^{-1} . \tag{51}$$

α is the viscosity parameter of standard accretion disks and $H(R)$ the height of the disk. Pressure equilibrium with a dipolar magnetosphere is then obtained at the radius $R_{\rm in}$

$$R_{\rm in} = 2.4\,R_* \left(\frac{\alpha\,I_{N+1}}{2}\right)^{2/7} \left(\frac{B_{*,3}\,R_*}{3R_\odot}\right)^{4/7} \left(\frac{H}{\dot{M}_{-7}\,R}\right)^{2/7} \left(\frac{R_* c^2}{10^6\,GM_*}\right)^{1/7} . \tag{52}$$

I_{N+1} is a structure parameter of order unity (Straumann, 1986). For accretion rates in the range of $\dot{M} \simeq 10^{-7}$ $\mathrm{M}_\odot$ yr^{-1}, the inner edge of such a disk is typically at a few stellar radii, provided the stellar magnetic field $B_* \simeq 10^3$ Gauss. The value for this inner edge of the accretion disk is only approximate, since the structure of the stellar magnetosphere is not exactly dipolar and the pressure in the disk can deviate from the standard Keplerian approximations. When the accretion rate increases considerably, the disk is driven towards the stellar surface, and the magnetic gap between stellar surface and the inner accretion disk completely disappears. When the accretion rate decreases, the magnetic gap will grow.

This kind of interaction between magnetic fields and accretion disks is extensively discussed in the case of accretion disks around magnetized neutron stars (Lamb, 1989). Since the boundary layer is highly turbulent, the magnetic field enters the disk on the diffusion time-scale $t_D = R_{\rm in}^2/\eta_T$, where $\eta_T \simeq P_m\,\nu_T$ and ν_T is the turbulent kinematic viscosity in the boundary layer

$$\nu_T \simeq \alpha\,\Omega\,H(R)^2 \simeq 10^{15}\,\alpha\ \mathrm{cm}^2\,\mathrm{s}^{-1} . \tag{53}$$

With these expressions we obtain a diffusion time scale given by the rotation period $P_{\rm in} \simeq$ days at the inner edge of the disk

$$t_D \simeq \frac{P_{\rm in}}{2\pi} \frac{1}{\alpha\,P_m} \left(\frac{H}{R}\right)^{-2} \simeq 30\,P_{\rm in} \left(\frac{10\,H}{R}\right)^{-2} \frac{1}{\alpha\,P_m} . \tag{54}$$

This is the fundamental time-scale for the evolution of fluctuations in the boundary layer. It essentially depends on the α-parameter and on the magnetic Prandtl number P_m.

The fast rotation in the disk generates electric radial fields in the disk, which drive a poloidal current system in the magnetosphere. These currents produce toroidal magnetic fields, which exert a momentum on the central star. The magnetic structure of this star-disk-system must then be calculated self-consistently including all the currents driven by the rotation. In a first approximation we neglect the influence of the plasma in the corona

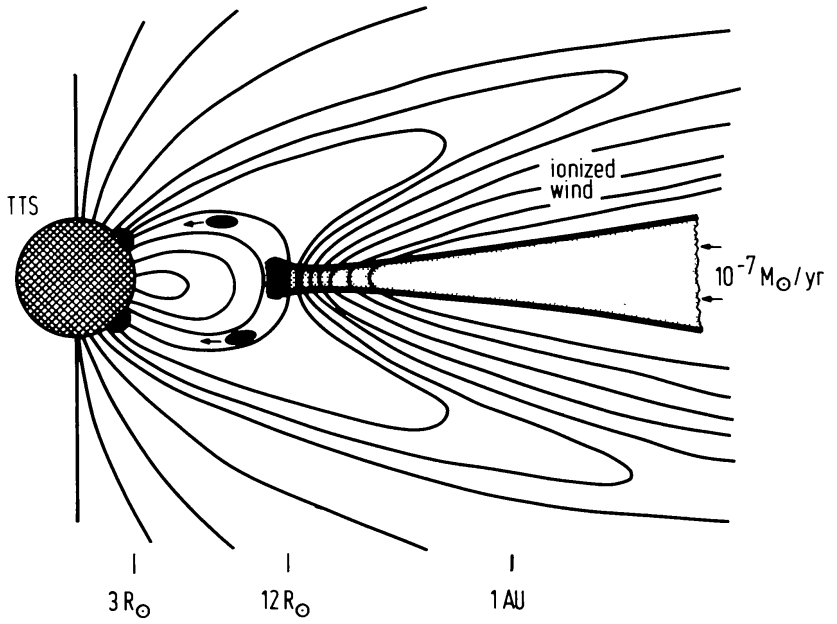

Fig. 12. The interaction between the rotating magnetosphere of the central star and the accretion disk in TTSs. The azimuthal motion of the plasma in the disk generates a radial electric field in the disk that drives the field aligned currents within the magnetosphere and cross-field currents in the disk and the corona of the star. The resulting magnetic torque density RB_ϕ is then negative in the upper hemisphere and positive in the lower hemisphere and acts to spin down the star. A strong wind is initiated along the open field lines emanating from the disk.

of the disk and the star. This means we can treat the problem in the force-free approximation. We can, however, not neglect the rapid rotation of the magnetosphere, since the light cylinder R_L is not at infinity

$$R_L = \frac{c}{\Omega_*} = \frac{c}{\omega \Omega_K(R_*)} = \frac{1}{\omega} R_* \left(\frac{R_* c^2}{GM_*}\right)^{1/2} \simeq 10^4 \, R_*/10\omega \simeq 10^{15} \text{ cm}/5\omega \,. \tag{55}$$

The light cylinder radius of T Tauri stars is typically at 100 AU, and the open part of the stellar magnetosphere is then confined inside the light cylinder radius. Since the outer part of the magnetosphere can only be closed outside the light cylinder, plasma flowing away along these field lines will open up the field structure with the result that now fields enter from the light cylinder and cross the disk (Fig. 12). Field lines emanating from beyond the corotation radius

$$R_{\rm cor} = \left(\frac{GM_*}{\Omega_*^2}\right)^{1/3} = R_* \left(\frac{R_L}{R_*}\right)^{2/3} \left(\frac{GM_*}{c^2 \, R_*}\right)^{1/3} \simeq 4.6 \, R_* \left(\frac{1}{10\omega}\right)^{2/3} \tag{56}$$

will carry wind plasma driven outwards centrifugally. In this domain, the force-free approximation is no longer correct and the plasma inertia should be included. Apart from this effect, we obtain a plasma carrying magnetosphere along the surface of the disk which is closed beyond the light cylinder

with field lines from inside the light cylinder. In this way, the field structure is globally closed, though the disk-wind blows up a magnetic bubble into the ambient medium. As is shown by Fig. 13, the disk-wind cannot be collimated to a radius smaller than the light cylinder - in fact the light cylinder is also here the natural scale for the jet-radius quite similar to the AGN jets.

Mundt et al. (1987) report jet radii for the ionized flows in the range of 10^{15} cm - 10^{16} cm. This is nicely in agreement with the jet radius being upto a factor 10 larger than the light cylinder. In fact, the jet will try to expand transversely until pressure equilibrium with the ambient molecular cloud is reached (see later on).

These magnetospheres also carry a current system. T Tauri stars are found to be in a kind of equilibrium state, where the angular momentum gain by mass accretion, $\dot{M}\sqrt{GM\,R_{\rm in}}$, is balanced by angular momentum loss through currents flowing from the star to the disk

$$\frac{dJ_*}{dt} = -\frac{1}{4\pi}\int_{\rm disk} RB_\phi\,\mathbf{B}_p\cdot d\mathbf{S} = -\frac{1}{c}\int I(\Psi)\,d\Psi \simeq -\frac{1}{c}\,I_{\rm max}\,\Psi_D\,. \qquad (57)$$

In the rotational equilibrium state, we need a current flow of the order of

$$I_{\rm max} = \frac{c^2}{\Psi_D}\,\dot{M}\,R_{\rm in}\sqrt{\frac{GM_*}{c^2\,R_{\rm in}}} \simeq 10^{14}\,{\rm Amp}\,\dot{M}_{-7}\,\Psi_{D,25}^{-1}\left(\frac{R_{\rm in}}{5R_*}\right)^{1/2}\,, \qquad (58)$$

corresponding to toroidal fields $\simeq 100$ Gauss at the surface of the star, or $\simeq 10$ Gauss at the inner edge of the disk. Such field strengths can be carried by the inner part of the disk. From pressure equilibrium between magnetic pressure and the disk pressure given by Eq. (51) we get the maximally possible disk field strength

$$B_\phi \simeq 42\,{\rm Gauss}\,\dot{M}_{-7}^{1/2}\,\alpha^{-1/2}\left(\frac{R_{\rm in}}{5R_*}\right)^{-5/4}\,. \qquad (59)$$

These fields are built up in the disk by differential rotation and dynamo effects (as discussed in Sec. 3). This rotational equilibrium which enforces $R_{\rm in} \simeq R_{\rm cor}$ solves the long-standing problem why accreting T Tauri stars are not rotating much faster. The observed slow rotation is especially surprising in view of the evidence for accretion from circumstellar disks in the pre-main sequence evolution. Accretion occurs at $\simeq 10^{-7}\,M_\odot$ yr^{-1} over a typical age of 10^6 years. In the absence of angular momentum loss, this would spin up a 1 $M_\odot$ star to about half the break-up speed (Hartmann and Stauffer, 1989). The magnetic coupling between star and disk provides then a natural explanation for the observed rotational velocities. The above model is also different from the one proposed by Shu et al. (1988), where

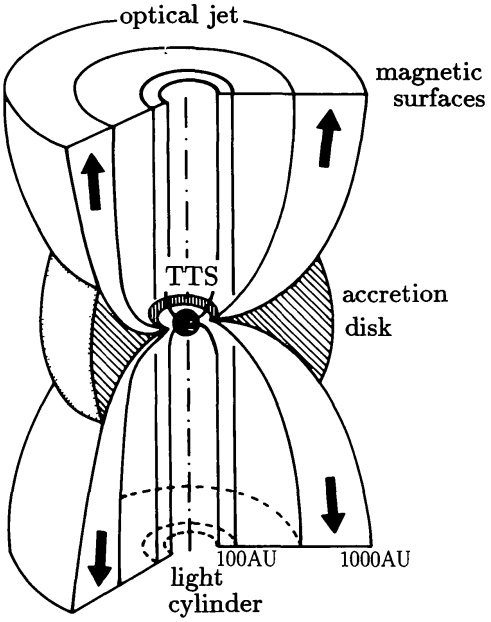

Fig. 13. The structure of magnetized T Tauri jets driven by the rapidly rotating magnetosphere. The magnetized disk-wind is collimated outside the light cylinder ($\simeq$ 50 AU, or less for younger objects) into bipolar jets with a typical radius of 500 AU. This is also the site of the origin of the forbidden lines in TTSs. The entire jet consists of a family of nested rotating magnetic surfaces which guide the plasma flow (arrows). Inside the light cylinder, the magnetic surfaces are closed to the stellar surface. They carry the return current

pre-main sequence stars rotate nearly at break-up because of high accretion from the disk, and bipolar outflows are driven away by this rapid rotation.

The disk-winds driven away by the rapid rotation of the magnetosphere are collimated outside the light cylinder of the central star into bipolar jets with a typical radius of 500 AU. Mundt et al. (1987, 1990) find a jet radius of a few 10^{15} cm in their sample, where the radius of the jet is estimated from the diameter of the optical knots. These jets consist of a family of nested magnetic surfaces, where the ionized wind flows between the surfaces (Fig. 13). The magnetic field is predominantly toroidal in this region with a field strength of $\simeq$ 1 milli-Gauss, corresponding to a current of 10^{14} Ampère. The terminal speed v_∞ in the jet follows from Eq. (40)

$$v_\infty \simeq V_m = 521\,\mathrm{km\,s^{-1}}\,\Psi_{*,25}^{2/3}\,R_{L,15}^{-2/3}\,\dot{M}_{w,-8}^{-1/3}\,. \tag{60}$$

This estimate is in nice agreement with the observed velocities in the optical jets of TTSs, $v_j \simeq 200 - 1000$ km s^{-1} (Mundt et al., 1990).

The mass flux in the jet, $\dot{M}_j$, and the kinetic luminosity L_j can be determined observationally, if the jet radius R_j, jet velocity v_p and density n_j in the jet are known (Mundt et al., 1987, 1990)

$$\dot{M}_j = 3.0 \times 10^{-9}\,M_\odot\,yr^{-1}\,R_{j,15.5}^2\,n_{j,2}\,v_{p,7.5}\,, \tag{61}$$

$$L_j = 8 \times 10^{-3}\,L_\odot\,\dot{M}_{j,-9}\,v_{p,7.5}^2\,. \tag{62}$$

The thermal pressure in the jet is at least one order of magnitude lower than the magnetic pressure ($n_j \leq 10^2$ cm^{-3}, the temperature $T_j \leq 10^4$ K, and therefore for the sound speed $c_S \simeq 10$ km/s). Since the sound speed in the jet is smaller than the magnetosonic speed in the jet,

$$v_{MS} = \sqrt{B^2/4\pi m_p n_j} \simeq 220\,\mathrm{km\,s^{-1}}\, B_{-3}\, n_{j,2}^{-1/2}\,, \tag{63}$$

strong protostellar jets are magnetically dominated, and the characteristic speed excited in the jet is the fast magnetosonic speed v_{FM}, defined as

$$v_{FM} = \frac{1}{\sqrt{2}}\left((v_{MS}^2 + c_S^2) + \sqrt{(v_{MS}^2 + c_S^2)^2 - 4\,c_S^2\,v_A^2}\right)^{1/2} \simeq c_S + v_{MS}\,. \tag{64}$$

Plasma flows therefore in the jet with a magnetosonic Mach number of $M_{FM} \simeq 1 - 5$ given by

$$M_{FM}^2 = \frac{4\pi m_p n_j v_p^2}{B^2} \simeq \frac{4\,\dot{M}_j\,v_p}{B^2\,R_j^2} \simeq \frac{\dot{M}_j\,c^2\,v_p}{I_{\max}^2} \simeq 1.6\,\dot{M}_{j,-8}\,v_{p,7.5}\,I_{14}^{-2}\,. \tag{65}$$

Whether the outflows will always reach super-magnetosonic speeds depends largely on the global topology of the magnetic surfaces.

The exact behaviour of the jet material only follows from self-consistent solutions of the Grad-Shafranov equation. All existing calculations for the stellar case have used quite strong simplifications in solving the transfield equation. Chan and Henriksen (1980), Blandford and Payne (1982) and Königl (1989) assumed self-similarity, Pudritz and Norman (1983) some special scaling with radius and Sakurai (1985, 1987) solved the transfield equation numerically only for a simplified initial monopole type geometry.

6. Conclusions

In this review, a unified discussion of hydromagnetic aspects of accretion disks in protostellar systems and the central region of galaxies has been given. These systems have been associated with collimated outflows which are most probably mediated by large scale poloidal magnetic fields that thread the central part of the disks. Jet generation can then be seen as a natural consequence of the magnetic activity of accretion disks. There are some extremely important issues which should be solved within the next years. The first is to investigate the dynamo problem for accretion disks including the backreaction of the magnetic fields on the evolution of the disk. Secondly, the large scale topology of the magnetic fields excited in accretion

disks has to be elaborated – dipolar fields behave differently from quadrupolar fields. Thirdly, stationary solutions of MHD wind magnetospheres should be enlarged to include also time–dependent evolution of non–axisymmetric flows.

Acknowledgements. The author would like to thank Prof. I. Appenzeller and Dr. T. Montmerle for stimulating discussions on the subject of T Tauri stars and to Dr. H. Lesch, S. Appl, M. Haehnelt and R. Khanna for general enlightening comments on the properties of magnetized plasmas. This work is supported by the Deutsche Forschungsgemeinschaft (SFB 328).

References

Abramowicz, M.A., Zurek, W.H.: 1981, *Astrophys. J.* **246**, 314
Alloin, D., Boisson, C., Pelat, D.: 1987, *Astron. Astrophys.* **200**, 17
Antonucci, R.R.J., Miller, J.S.: 1985, *Astrophys. J.* **297**, 621
Appenzeller, I.: 1989, in *Modeling the Stellar Environment*, ed. P. Delache (Editions Frontières, Paris), p. 47
Appenzeller, I., Mundt, R.: 1989, *Astron. Astrophys. Review* **1**, 291
Appl, S.: 1990, *Ph. D. thesis*, University of Heidelberg
Barthel, P.: 1989, *Astrophys. J.* **336**, 606
Beckwith, S.V.W., Sargent, A.I., Chini, R., Güsten, R.: 1990, *Astron. J.* **99**, 924
Benford, G.: 1978, *Mon. Not. Roy. Astron. Soc.* **183**, 29
Benford, G.: 1987, in *Astrophysical Jets and their Engines*, ed. W. Kundt, NATO Advanced Science Institute **208**, Reidel (Dordrecht), p. 197
Bertout, C.: 1989, *Ann. Rev. Astron. Astrophys.* **27**, 351
Biretta, J.A., Moore, R.L., Cohen, M.H.: 1986, *Astrophys. J.* **308**, 93
Blandford, R.D.: 1989, in *Theory of Accretion Disks*, eds. F. Meyer, W.J. Duschl, J. Frank and E. Meyer-Hofmeister, Kluwer (Dordrecht), p. 35
Blandford, R.D., Payne, D.G.: 1982, *Mon. Not. Roy. Astron. Soc.* **199**, 883
Brandenburg, A., Tuominen, I., Krause, F.: 1990, *Geophys. Astrophys. Fluid Dyn.* **50**, 95
Breuer, R.A.: 1975, *Lecture Notes in Physics* (Springer, Berlin) **44**
Bridle, A.H., Perley, R.: 1984, *Ann. Rev. Astron. Astrophys.* **22**, 319
Camenzind, M.: 1986a, *Astron. Astrophys.* **156**, 137
Camenzind, M.: 1986b, *Astron. Astrophys.* **162**, 32
Camenzind, M.: 1987a, *Astron. Astrophys.* **184**, 341
Camenzind, M.: 1987b, in *Interstellar Magnetic Fields*, eds. R. Beck and R. Gräve, Springer (Berlin), p. 229
Camenzind, M.: 1988, in *High Energy Astrophysics*, ed. G. Börner, Springer Proceedings, Springer (Berlin), p. 118
Camenzind, M.: 1989a, in *Theory of Accretion Disks*, eds. F. Meyer, W.J. Duschl, J. Frank and E. Meyer-Hofmeister, Kluwer (Dordrecht), p. 59
Camenzind, M.: 1989b, in *Accretion Disks and Magnetic Fields in Astrophysics*, ed. G. Belvedere, Kluwer (Dordrecht), p. 129
Camenzind, M.: 1990a, in *IAU Symp. 140: Galactic and Intergalactic Magnetic Fields*, eds. R. Beck, P.P. Kronberg, R. Wielebinski, Reidel (Dordrecht), p. 413
Camenzind, M.: 1990b, Habilitation, Univ. Heidelberg
Camenzind, M.: 1990c, in preparation
Camenzind, M., Endler, M.: 1990, in preparation
Camenzind, M., Lesch, H.: 1990, in preparation

Chan, K.L., Henriksen, R.N.: 1982, *Astrophys. J.* **241**, 534
Chen, K., Halpern, J.P., Filippenko, A.V.: 1989, *Astrophys. J.* **339**, 742
Cohen, M.H., Zensus, J.A., Biretta, J.A., Comoretto, G., Kaufmann, P., Abraham, Z.: 1987, *Astrophys. J.* **315**, L89
Collin-Souffrin, S.: 1987, *Astron. Astrophys.* **179**, 60
Coroniti, F.V.: 1985, in *Unsteady Current Systems in Astrophysics, IAU Symp.* **107**, eds. M.R. Kundu and G.D. Holman, Reidel (Dordrecht), p. 453
Courvoisier, T.J.-L., Camenzind, M.: 1989, *Astron. Astrophys.* **224**, 10
Draine, B.T.: 1983, *Astrophys. J.* **270**, 519
Edwards, S., Cabrit, S., Ghandour, L.O., Strom, S.E.: 1989, in *ESO Workshop on Low Mass Star Formation and Pre-Main Sequence Objects*, ed. Bo Reipurth, ESO Proceedings **33**, 385
Elvis, M., Lawrence, A.: 1988, *Astrophys. J.* **331**, 161
Fukui, Y.: 1989, in *ESO Workshop on Low Mass Star Formation and Pre-Main Sequence Objects*, ed. Bo Reipurth, ESO Proceedings **33**, 95
Haehnelt, M., Camenzind, M.: 1990, in preparation
Halpern,J.P., Filippenko, A.V.: 1988, *Nature* **331**, 46
Hartmann, L., Stauffer, J.R.: 1989, *Astron. J.* **97**, 873
Hartmann, L., MacGregor, K.B.: 1982, *Astrophys. J.* **259**, 180
Hessman, F.V., Eislöffel, J., Mundt, R., Hartmann, L., Herbst, W., Krautter, J.: 1990, submitted to *Astrophys. J.*
Heyvaerts, J., Norman, C.A.: 1989, *Astrophys. J.* **347**, 1055
Heyvaerts, J., Priest, E.R.: 1989, *Astron. Astrophys.* **216**, 230
Kawara, K., Nishida, M., Gregory, B.: 1990, *Astrophys. J.* **352**, 433
Khanna, R., Camenzind, M.: 1990, in preparation
Kley, W.: 1989, *Astron. Astrophys.* **208**, 98
Kley, W.: 1990, this volume
Königl, A.: 1990, *Astrophys. J.* **342**, 208
Kössl, D., Müller, E., Hillebrandt, W.: 1989, *Astron. Astrophys.* **229**, 378
Koyama, K.: 1989, in *IAU Symposium 134, Active Galactic Nuclei*, eds. D.E. Osterbrock and J.S. Miller, Kluwer (Dordrecht), p. 167
Krause, F., Meinel, R., Elstner, D., Rüdiger, G.: 1990, in *IAU Symp. 140: Galactic and Intergalactic Magnetic Fields*, eds. R. Beck, P.P. Kronberg, R. Wielebinski, Reidel (Dordrecht), p. 97
Krause, F., Rädler, K.-H.: 1980, *Mean Field Magnetohydrodynamics and Dynamo Theory*, Pergamon Press (Oxford)
Krichbaum, T.P. et al.: 1990, MPIfR preprint, submitted to *Astron. Astrophys.*
Krolik, J.H., Begelman, M.C.: 1988, *Astrophys. J.* **329**, 702
Lada, C.J.: 1985, *Ann. Rev. Astron. Astrophys.* **23**, 267
Lamb, F.K.: 1989, in *Timing Neutron Stars*, eds. H. Ögelman and E.P.J. van den Heuvel, Kluwer (Dordrecht), p. 649
Laor, A., Netzer, H.: 1989, *Mon. Not. Roy. astron. Soc.* **238**, 897; **242**, 560
Lesch, H., Appl, S., Camenzind, M.: 1989, *Astron. Astrophys.* **225**, 341
Lind, K.R., Payne, D.G., Meier, D.L., Blandford, R.D.: 1989, *Astrophys. J.* **344**, 89
Lovelace, R.V.E., Wang, J.C.L., Sulkanen, M.E.: 1987, *Astrophys. J.* **315**, 504
Malkan, M.: 1989, in *Theory of Accretion Disks*, eds. F. Meyer, W.J. Duschl, J. Frank and E. Meyer-Hofmeister, Kluwer (Dordrecht), p. 19
Matsumoto, R., Horiuchi, T., Hanawa, T., Shibata, K.: 1990, *Astrophys. J.* **356**, 259
Michel, F.C.: 1969, *Astrophys. J.* **157**, 1183
Michel, F.C.: 1982, *Rev. Mod. Phys.* **54**, 1
Moffatt, H.K.: 1978, *Magnetic Field Generation in Electrically Conducting Fluids*, Cambridge Univ. Press (Cambridge)
Montmerle, T., André, P.: 1988, in *Formation and Evolution of Low Mass Stars*, eds. A.K. Dupree and M.T.V.T. Lago (Kluwer, Dordrecht), p. 225
Mundt, R.: 1988, in *Formation and Evolution of Low Mass Stars*, eds. A.K. Dupree and M.T.V. Lago (Kluwer, Dordrecht), p. 257
Mundt, R., Brugel, E.W., Bührke, T.: 1987, *Astrophys. J.* **319**, 275
Mundt, R., Ray, T.P., Bührke, T., Raga, A.C., Solf, J.: 1990, *Astron. Astrophys.* **232**, 37

Parker, E.N.: 1971, *Astrophys. J.* **163**, 255
Perley, R.: 1989, in *Hot Spots in Extragalactic Radio Sources*, eds. K. Meisenheimer and H.-J. Röser, Lecture Notes in Physics (Springer, Berlin) **327**, 1
Poetzel, R., Mundt, R., Ray, T.P.: 1989, *Astron. Astrophys.* **224**, L13
Porcas, R.W.: 1987, in *Superluminal Radio Sources*, Eds. J.A. Zensus and T.J. Pearson, Cambridge University Press (Cambridge), p. 12
Pringle, J.: 1989, *Mon. Not. Roy. Astron. Soc.* **236**, 107
Pudritz, R.E.: 1981, *Mon. Not. R. astr. Soc.* **195**, 881; 897
Pudritz, R.: 1989, in *Galactic and Extragalactic Star Formation*, eds. R.E. Pudritz and M. Fich (Kluwer, Dordrecht), p. 135
Pudritz, R.E., Norman, C.A.: 1983, *Astrophys. J.* **274**, 677
Pudritz, R.E., Norman, C.A.: 1986, *Astrophys. J.* **301**, 571
Rüdiger, G.: 1990, *Geophys. Astrophys. Fluid Dynamics* **50**, 53
Ruzmaikin, A.A., Shukurov, A.M., Sokoloff, D.D.: 1988, *Magnetic Fields of Galaxies*, Kluwer (Dordrecht)
Sakurai, T.: 1985, *Astron. Astrophys.* **152**, 121
Sakurai, T.: 1987, *Publ. astron. Soc. Japan* **39**, 821
Sanders, D.B., Phinney, E.S., Neugebauer, G., Soifer, B.T., Matthews, K.: 1989, *Astrophys. J.* **347**, 29
Scharleman, E.T., Wagoner, R.V.: 1973, *Astrophys. J.* **182**, 951
Shakura, N.I., Sunyaev, R.A.: 1973, *Astron. Astrophys.* **24**, 337
Shibata, K., Tajima, T., Matsumoto, R., Horiuchi, T., Hanawa, T., Rosner, R., Uchida, Y.: 1989, *Astrophys. J.* **338**, 471
Shu, F.H., Lizano, S., Adams, F.C.: 1987, *Ann. Rev. Astron. Astrophys.* **25**, 23
Shu, F.H., Lizano, S., Ruden, S.P., Najita, L.: 1988, *Astrophys. J. Letters* **328**, L19
Stirpe, G.M., deBruyn, A.G., von Groningen, E.: 1988, *Astron. Astrophys.* **200**, 9
Straumann, N.: 1986, *General Relativity and Relativistic Astrophysics*, Texts and Monographs in Physics, Springer (Berlin)
Strom, S.E., Strom, K.M., Edwards, S.: 1988, in *Proc. NATO Advanced Study Institute on Galactic and Extragalactic Star Formation*, eds. R.E. Pudritz and M. Fich (Kluwer, Dordrecht), p. 53
Sun, W.-H., Malkan, M.: 1989, *Astrophys. J.* **346**, 68
Tylenda, R.: 1981, *Acta Astron.* **31**, 267
Ulrich, M.-H.: 1989, in *Theory of Accretion Disks*, eds. F. Meyer, W.J. Duschl, J. Frank and E. Meyer-Hofmeister, Kluwer (Dordrecht), p. 3
Walker, R.C., Benson, J.M., Unwin, S.C.: 1987, *Astrophys. J.* **316**, 546
Zel'dovich, Ya.B., Ruzmaikin, A.A., Sokoloff, D.D.: 1983, *Magnetic Fields in Astrophysics*, Pergamon Press (Oxford)
Zensus, J.A.: 1989, in *BL Lac Objects*, eds. L. Maraschi, T. Maccacaro, M.-H. Ulrich, Lecture Notes in Physics (Springer, Berlin) **334**, 3